

## TO THE EDITOR:

Normalizing hepcidin predicts *TMPRSS6* mutation status in patients with chronic iron deficiency

Matthew M. Heeney,<sup>1-3</sup> Dongjing Guo,<sup>3</sup> Luigia De Falco,<sup>4,5</sup> Dean R. Campagna,<sup>6</sup> Gordana Olbina,<sup>7</sup> Paige P.-C. Kao,<sup>3</sup> Klaus Schmitz-Abe,<sup>8</sup> Fedik Rahimov,<sup>9</sup> Patrick Gutschow,<sup>7</sup> Keith Westerman,<sup>7</sup> Vaughn Ostland,<sup>7</sup> Tracy Jackson,<sup>10</sup> Robert J. Klaassen,<sup>10</sup> Kyriacos Markianos,<sup>6</sup> Karin E. Finberg,<sup>11</sup> Achille Iolascon,<sup>4,5</sup> Mark Westerman,<sup>7</sup> Wendy B. London,<sup>1-3</sup> and Mark D. Fleming<sup>6</sup>

<sup>1</sup>Division of Hematology/Oncology, Boston Children's Hospital, Boston, MA; <sup>2</sup>Dana-Farber Cancer Institute, Boston, MA; <sup>3</sup>Dana-Farber/Boston Children's Cancer and Blood Disorders Center, Harvard Medical School, Boston, MA; <sup>4</sup>Department of Molecular Medicine and Medical Biotechnologies, Federico II University Medical School, Naples, Italy; <sup>5</sup>CEINGE Biotechnologie Avanzate, Naples, Italy; <sup>6</sup>Department of Pathology, Boston Children's Hospital, Boston, MA; <sup>7</sup>Intrinsic LifeSciences, La Jolla, CA; <sup>8</sup>Division of Newborn Medicine, and <sup>9</sup>Division of Genetics and Genomics, Department of Medicine, Boston Children's Hospital, Boston, MA; <sup>10</sup>Division of Pediatric Hematology-Oncology, Children's Hospital of Eastern Ontario, Ottawa, ON, Canada; and <sup>11</sup>Department of Pathology, Yale University, New Haven, CT

Iron-refractory iron deficiency anemia (IRIDA) is characterized by congenital iron deficiency (ID) that is poorly responsive to oral iron treatment. Biallelic mutations in *TMPRSS6* are found in most patients with IRIDA.<sup>1</sup> *TMPRSS6* negatively regulates synthesis of the iron regulatory hormone hepcidin, and loss of *TMPRSS6* causes inappropriately elevated plasma hepcidin and impaired iron absorption and recycling.<sup>2</sup> IRIDA can be difficult to distinguish from complicated cases of acquired iron deficiency that are unresponsive to oral or parenteral iron therapy. We sought to develop an algorithm based on blood and plasma values to distinguish patients with IRIDA resulting from biallelic *TMPRSS6* mutations (*TMPRSS6*<sup>mut/mut</sup>) from patients with chronic iron deficiency (cID) unrelated to *TMPRSS6*. To do this, we analyzed the hematologic, biochemical, and genetic features of a group of patients (n = 139) with cID/anemia (cID/A) referred for research testing for *TMPRSS6* mutations (supplemental Figure 1, available on the *Blood* Web site).

Because the diagnosis of IRIDA might be considered only in patients with iron deficiency, we restricted our analysis to individuals with transferrin saturation (TfSat) ≤15% at the time of the study (Table 1). Hypoferritinemia was not used as an inclusion criterion because it is not a reliable indicator of ID in IRIDA patients. Compared with wild-type controls, heterozygosity for a *TMPRSS6* mutation (*TMPRSS6*<sup>mut/+</sup>) was associated with significant changes in mean cell volume and plasma iron, ferritin, and hepcidin, confirming a mild *TMPRSS6*<sup>mut/+</sup> phenotype. As a group, the patients with biallelic *TMPRSS6* mutations were slightly more anemic and iron deficient than patients in the cID group. Despite the apparent relative ID, *TMPRSS6*<sup>mut/mut</sup> individuals had a reduced total iron binding capacity compared with those in the *TMPRSS6*<sup>+/+</sup> group and a higher plasma ferritin than those in the cID group (supplemental Figure 2). In comparison with iron-replete *TMPRSS6*<sup>+/+</sup> controls and patients in the cID group, plasma hepcidin was significantly increased in *TMPRSS6*<sup>mut/mut</sup> patients ( $P < .0001$ ; Table 1; Figure 1). Hepcidin is characteristically decreased in ID<sup>3</sup>; however, we found a lower median but a similar mean in the cID group compared with controls (Table 1), suggesting a physiological reason for the relative iron refractoriness of some individuals in this group. Indeed, several of these patients had a high C-reactive protein, indicative of

inflammation, which can stimulate hepcidin production (supplemental Tables 1 and 4).

Receiver operating characteristic curve analysis of plasma hepcidin levels showed an area under the curve (AUC) of 0.861 in the ability of hepcidin to distinguish the *TMPRSS6*<sup>mut/mut</sup> and cID groups (Figure 1D; supplemental Table 4), which was better than a similar analysis of ferritin (AUC, 0.767; Figure 1D; supplemental Figure 2C). Thus, measurement of plasma hepcidin alone can facilitate the discrimination of patients with IRIDA resulting from biallelic *TMPRSS6* mutations from patients with cID/A unrelated to *TMPRSS6*. Nevertheless, because there was significant overlap in hepcidin levels between the *TMPRSS6*<sup>mut/mut</sup> and cID groups, *TMPRSS6*<sup>mut/+</sup> individuals, and controls (Figure 1A), we sought to evaluate hepcidin derivative indices to distinguish these groups.

The hepcidin:ferritin ratio has been used to attempt to normalize hepcidin for iron stores.<sup>4</sup> We found that the plasma hepcidin:ferritin ratio is a poor predictor of *TMPRSS6* mutation status in patients with cID (AUC, 0.571; Table 1; Figure 1D; supplemental Figure 2D). We reasoned that normalization of hepcidin to the plasma iron or TfSat might be more physiologically relevant, because it is thought that hepcidin is responsive to the plasma concentration of diferric transferrin. The iron/log<sub>10</sub>(hepcidin) and TfSat/log<sub>10</sub>(hepcidin) ratios correlated with *TMPRSS6* mutation status in iron-deficient patients (Table 1; Figure 1B-C). Plasma iron/log<sub>10</sub>(hepcidin) (AUC, 0.930) seems to be superior to TfSat/log<sub>10</sub>(hepcidin) (AUC, 0.886) in terms of ability to discriminate cID patients from *TMPRSS6*<sup>mut/mut</sup> patients (Figure 1D). At a fixed sensitivity of 80%, both plasma iron/log<sub>10</sub>(hepcidin) and TfSat/log<sub>10</sub>(hepcidin) had superior specificity (91%; 95% confidence interval [CI], 78%-97% and 89%; 95% CI, 75%-95%, respectively) than plasma hepcidin alone (77%; 95% CI, 62%-99%) (supplemental Table 3). The correlation between hepcidin and ferritin suggested that substitution of ferritin for hepcidin in either of these quotients could yield a comparably sensitive and specific relationship. Of these, the iron/log<sub>10</sub>(ferritin) gave the best performance characteristics, with an AUC of .911 and a specificity of 91% (95% CI, 78%-97%) at a sensitivity of 80% (supplemental Table 3).

**Table 1. Comparison of patients' hematologic and iron metabolism characteristics and derivative hepcidin and ferritin indices**

	No.	Mean	Minimum	Maximum	Median	SD	SEM	Wilcoxon signed rank test 2-tailed P		
								vs mut/mut	vs cID	vs +/+
<b>Age (y)</b>										
mut/mut	43*	13	1	50	10	12	2			
cID	57	23	1	69	16	21	3	.0006		
+/+	31	38	2	90	41	22	4	<.0001	.2886	
mut/+	64	37	3	73	39	18	2	<.0001	<.0001	.5574
<b>Hemoglobin (g/dL)</b>										
mut/mut	43*	9.0	5.7	11.7	8.8	1.3	0.2			
cID	59	9.8	3.6	13.3	10.1	2.1	0.3	.0005		
+/+	35	14.1	12.2	15.9	14.0	1.1	0.2	<.0001	<.0001	
mut/+	65	13.5	8.7	16.5	13.6	1.5	0.2	<.0001	<.0001	.018
<b>Mean red blood cell volume (fL)</b>										
mut/mut	43*	61.2	50.0	75.1	60.0	6.3	1.0			
cID	59	72.3	55.6	96.2	72.1	8.9	1.2	<.0001		
+/+	35	90.1	77.1	99.7	90.1	5.1	0.9	<.0001	<.0001	
mut/+	65	86.1	68.1	107.3	86.2	6.7	0.8	<.0001	<.0001	<.0001
<b>Iron (μg/dL)</b>										
mut/mut	44	19	11	44	17	7	1			
cID	59	30	12	72	26	14	2	<.0001		
+/+	35	86	35	126	87	27	5	<.0001	<.0001	
mut/+	66	74	15	176	70	35	4	<.0001	<.0001	.0017
<b>Total iron binding capacity (μg/dL)</b>										
mut/mut	44	365	182	503	359	67	10			
cID	59	433	186	626	442	98	13	<.0001		
+/+	35	404	311	564	392	74	12	.0028	.0046	
mut/+	66	386	179	556	387	69	9	.0007	<.0001	.3558
<b>Transferrin saturation (%)</b>										
mut/mut	44	5	3	13	5	3	0			
cID	59	7	2	15	7	4	0	<.0001		
+/+	35	23	8	41	21	9	2	<.0001	<.0001	
mut/+	66	20	3	56	20	11	1	<.0001	<.0001	.2729
<b>Ferritin (ng/mL)</b>										
mut/mut	44	96.9	2.8	511.4	66.2	100.2	15.1			
cID	59	51.9	1.3	636.0	10.2	106.5	13.9	.0004		
+/+	35	78.3	5.9	302.0	43.3	78.1	13.2	.7524	<.0001	
mut/+	66	115.8	2.7	536.4	70.9	117.3	14.4	.0183	<.0001	<.0001
<b>Zinc protoporphyrin:heme ratio (μmol/mol)</b>										
mut/mut	24	120	474	253	249	99	20			
cID	45	33	605	206	180	136	20	.0069		
+/+	34	24	103	46	43	15	3	<.0001	<.0001	
mut/+	61	21	344	62	46	53	7	<.0001	<.0001	.0081

+/+, wild-type controls; cID, no *TMPRSS6* mutations detected; mut/+, clinically unaffected *TMPRSS6* heterozygotes; mut/mut, biallelic *TMPRSS6* mutations detected; SD, standard deviation; SEM, standard error of the mean.

\*A concurrent complete blood count was not available for 1 patient.

**Table 1. (continued)**

	No.	Mean	Minimum	Maximum	Median	SD	SEM	Wilcoxon signed rank test 2-tailed P		
								vs mut/mut	vs cID	vs +/+
<b>Serum transferrin receptor (mg/L)</b>										
mut/mut	19	14.53	5.18	28.82	15.19	5.23	1.2			
cID	28	15.26	3.45	62.56	9.52	14.14	2.67	.33		
+/+	23	3.75	2.3	8.45	3.23	1.49	0.31	<.0001	<.0001	
mut/+	51	4.11	1.89	14.77	3.63	2.17	0.30	<.0001	<.0001	.0066
<b>C-reactive protein (mg/L)</b>										
mut/mut	42	0.15	0.03	2.06	0.09	0.34	0.05			
cID	58	0.35	0.03	4.20	0.10	0.73	0.10	.0046		
+/+	35	0.31	0.03	2.32	0.10	0.54	0.09	.003	.0069	
mut/+	63	0.37	0.03	4.10	0.10	0.8	0.10	.0005	.0015	.0015
<b>Hepcidin (ng/mL)</b>										
mut/mut	44	69.7	8.8	219.3	62.8	45.5	6.9			
cID	59	21.5	2.8	105.1	7.0	27.7	3.6	<.0001		
+/+	35	20.8	4.1	76.9	14.8	17.3	2.9	<.0001	<.0001	
mut/+	66	28.5	2.9	91.8	23.6	18.8	2.3	<.0001	<.0001	<.0001
<b>Iron/log(ferritin)</b>										
mut/mut	44	11.3	6.5	31.3	9.2	5.7	0.9			
cID	59	31.2	6.4	122.9	28.5	18.9	2.5	<.0001		
+/+	35	53.8	19.9	99.9	51.6	18.4	3.1	<.0001	<.0001	
mut/+	66	40.9	12.1	103.0	39.0	19.0	2.3	<.0001	<.0001	<.0001
<b>Transferrin saturation/ log(ferritin)</b>										
mut/mut	44	3.2	1.7	8.8	2.7	1.7	0.3			
cID	59	7.1	2.0	23.9	6.5	3.5	0.5	<.0001		
+/+	35	13.6	4.6	26.9	13.2	4.9	0.8	<.0001	<.0001	
mut/+	66	11.0	3.0	32.8	11.0	5.6	0.7	<.0001	<.0001	.0004
<b>Hepcidin/ferritin</b>										
mut/mut	44	1.3	0.1	6.8	1.0	1.3	0.2			
cID	59	1.2	0.1	10.8	0.8	1.6	0.2	.4183		
+/+	35	0.4	0.1	1.4	0.3	0.3	0	<.0001	<.0001	
mut/+	66	0.5	0.0	2.6	0.3	0.5	0.1	<.0001	<.0001	.0533
<b>Iron/log(hepcidin)</b>										
mut/mut	44	11.1	5.3	30.2	9.7	5.2	0.8			
cID	59	32.1	7.0	80.9	27.2	17.8	2.3	<.0001		
+/+	35	77.1	26.6	169	69.7	29.8	5.0	<.0001	<.0001	
mut/+	66	57.7	9.4	170.8	49.9	32.0	3.9	<.0001	<.0001	.0003
<b>Transferrin saturation/ log(hepcidin)</b>										
mut/mut	44	3.2	1.4	8.9	2.5	1.8	0.3			
cID	59	7.5	2.1	19.2	6.2	4.0	0.5	<.0001		
+/+	35	19.6	6.2	40.2	18.1	8.0	1.3	<.0001	<.0001	
mut/+	66	15.8	2.3	48.8	13.9	9.9	1.2	<.0001	<.0001	.0058

+/+, wild-type controls; cID, no *TMPRSS6* mutations detected; mut/+, clinically unaffected *TMPRSS6* heterozygotes; mut/mut, biallelic *TMPRSS6* mutations detected; SD, standard deviation; SEM, standard error of the mean.

\*A concurrent complete blood count was not available for 1 patient.

To compare the hepcidin and ferritin indices, we developed 2 multivariable models, 1 based on hepcidin and the other on ferritin, each normalized to iron and TfSat. Significant variables

were identified by using univariable logistics (supplemental Table 4); thereafter, we obtained 2 multivariable models (supplemental Table 5).

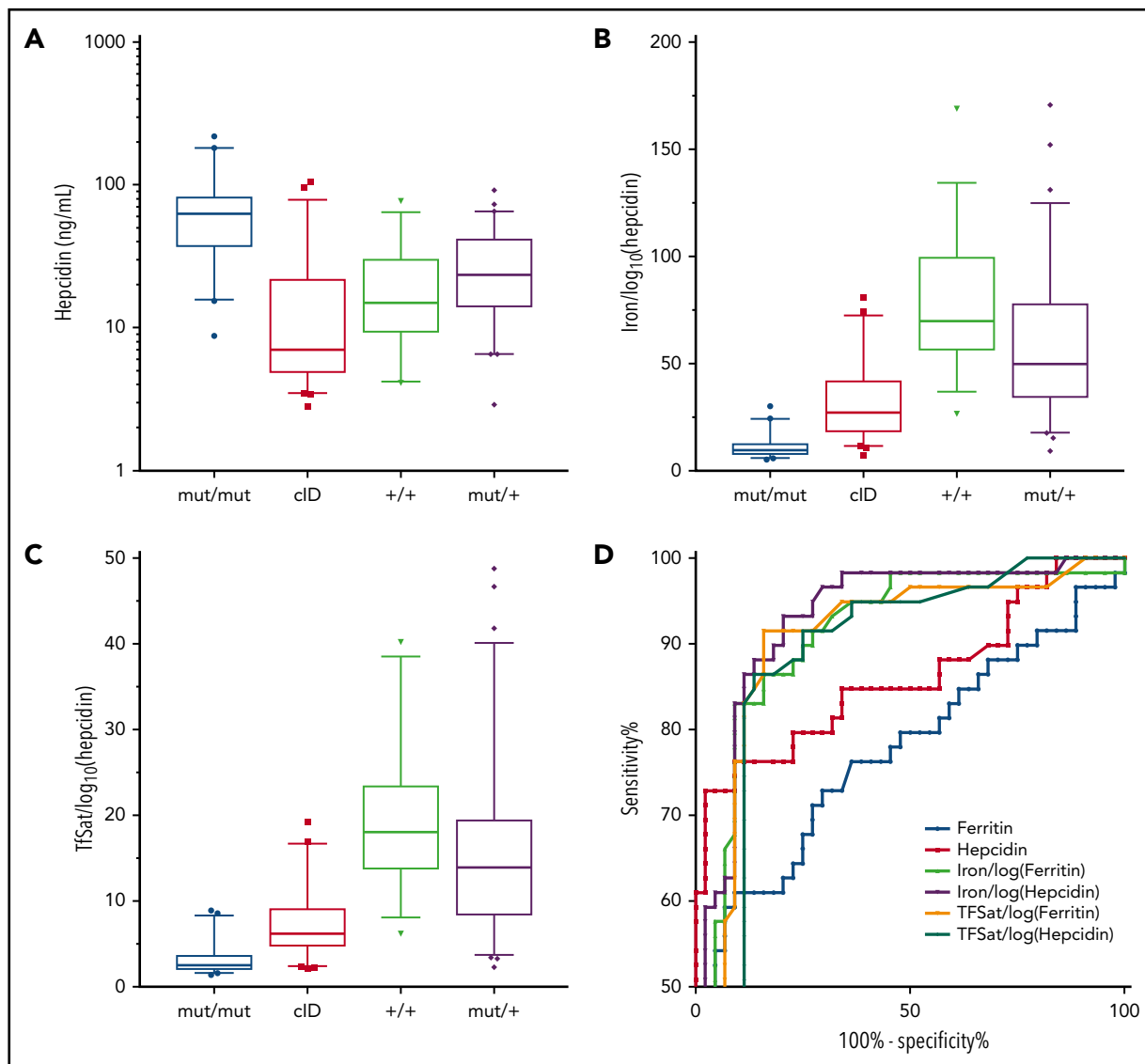


**Figure 1. Plasma hepcidin and derivative indices in iron metabolism disorders.** (A-C) Plasma hepcidin and derivative indices of IRIDA patients with biallelic *TMPRSS6* mutations (*mut/mut* [n = 44]), their heterozygous relatives (*mut/+* [n = 59]), wild-type controls (*+/+* [n = 35]), and *TMPRSS6*-mutation-negative cID/A patients (cID [n = 66]). Box and whisker plots present the quartiles (box), and the 10th and 90th percentiles (whiskers). (D) Receiver operating characteristic curve analysis comparing hepcidin, ferritin, and their derivative indices in the *TMPRSS6*<sup>mut/mut</sup> and cID groups (see also supplemental Tables 2 and 3; supplemental Figure 2).

$$\text{Model 1: } \text{Logit}(p) = 10.0744 - 0.6543 \cdot \text{HGB} - 0.2412 \cdot \text{Iron}/\log_{10}(\text{Ferritin})$$

$$\text{Model 2: } \text{Logit}(p) = 9.7743 - 0.7826 \cdot \text{HGB} + 0.2067 \cdot \text{Iron} - 0.4487 \cdot \text{Iron}/\log_{10}(\text{Hepcidin})$$

where

$$\text{Logit}(p) = \log\left(\frac{1}{1-p}\right)$$

and  $p$  is the probability of a patient having 2 pathogenic *TMPRSS6* alleles.

Taken together, these data suggest that measurements of hepcidin or ferritin in combination with the plasma iron and hemoglobin can predict biallelic *TMPRSS6* mutations in individuals with cID/A.

We and others have consistently identified only 1 pathogenic allele in a subset of patients presenting with IRIDA.<sup>5</sup> To address

whether these individuals have an occult *TMPRSS6* mutation, we determined the ability of the metrics described above to predict the genotype of iron-deficient (TfSat  $\leq 15\%$ ) *TMPRSS6*<sup>mut/+</sup> relatives of *TMPRSS6*<sup>mut/mut</sup> patients (supplemental Table 6). The iron/log<sub>10</sub>(hepcidin) and the iron/log<sub>10</sub>(ferritin) were the most sensitive metrics for discriminating these groups, both having a sensitivity of 93% (95% CI, 76%-99%) with specificity of 90% (95% CI, 78%-97%). We used these cutoff values to determine whether 11 iron-deficient patients with 1 discoverable *TMPRSS6* allele were more likely to be phenotypically affected heterozygotes or compound heterozygotes (supplemental Table 7). Using the iron/log<sub>10</sub>(hepcidin) and the iron/log<sub>10</sub>(ferritin) measurements, 2 and 3 of the 11 patients were predicted to be a clinically affected heterozygotes, respectively; multivariable models 1 and 2 also predicted the same 2 and 3 patients to be affected heterozygotes. In all cases, as one might expect from the co-inheritance of a mutant allele and the same *TMPRSS6* haplotype on the other allele, 3 pairs of genotypically concordant

siblings were predicted to carry 2 mutant *TMPRSS6* alleles. Thus, in many cases, it is highly likely that clinically affected individuals with 1 *TMPRSS6* pathogenic variant possess a second occult mutant allele.

While this manuscript was in preparation, another group of investigators also studied the utility of normalizing plasma hepcidin to the TfSat in patients with IRIDA.<sup>6</sup> In particular, they compared the TfSat:hepcidin ratio in *TMPRSS6*-mutated patients who had 1 or 2 mutated alleles and found that, in general, those individuals with a single detectable allele had a milder biochemical phenotype than those with 2 mutated alleles. We suggest that most patients with a severe clinical phenotype likely have biallelic *TMPRSS6* mutations and that, in some cases, the second allele is genetically occult.

One goal of this study was to elaborate a biochemical method that might predict which patients in a group of individuals with cID/A were most likely to have biallelic *TMPRSS6* mutations. The study group included only those who were poorly responsive to oral iron and had a TfSat  $\leq 15\%$ , that is to say, those who had a higher pretest probability of having IRIDA as a result of *TMPRSS6* mutations than an unselected group with ID/A and TfSat  $\leq 15\%$ . Application of these tests in a broader iron-deficient population would likely result in a lower specificity. Nonetheless, one might argue that, regardless of whether or not an individual with cID/A has *TMPRSS6* mutations, a relative hepcidin excess, as indicated by the normalized hepcidin or ferritin ratios or multivariable model would indicate that they would benefit from early initiation of parenteral iron therapy.

## Acknowledgments

The authors thank the multitude of astute clinicians who referred individual patients and families to us for the evaluation of ID/A (see supplemental Acknowledgments). Likewise, the willing participation of the patients and their family members was essential to the successful completion of this study. The authors acknowledge Susan Wong and Megan Towne for coordinating sample shipments and maintaining study records.

This study was supported by grant No. R44 DK083843 from the National Institutes of Health, National Institute of Diabetes and Digestive and Kidney Diseases (M.W. and M.D.F.) and K12 HL087164 from the National Institutes of Health, National Heart, Lung, and Blood Institute (M.M.H.).

## Authorship

Contribution: M.M.H., M.W., and M.D.F. conceived of the study; M.M.H., L.D.F., R.J.K., T.J., K.E.F., A.I., and M.D.F. evaluated patient characteristics;

L.D.F., D.R.C., K.S.-A., F.R., K.M., A.I., and M.D.F. performed or interpreted genetic analyses; D.G. and W.B.L. designed and performed statistical analyses; P.P.-C.K. helped perform statistical analyses; G.O., K.W., P.G., V.O., and M.W. developed and performed the hepcidin immunoassay; and M.M.H., M.W., W.B.L., and M.D.F. prepared the initial draft of the manuscript, which was substantially edited by K.E.F. and reviewed by all authors.

Conflict-of-interest disclosure: G.O., P.G., K.W., V.O., and M.W. are or were employees of Intrinsic LifeSciences. G.O., K.W., and V.O. hold ownership interest in the company. M.W. served as president and chief executive officer. The remaining authors declare no competing financial interests.

Mark Westerman died on 30 August 2017.

ORCID profiles: M.M.H., 0000-0002-1104-6843; M.D.F., 0000-0003-0948-4024.

Correspondence: Mark D. Fleming, Department of Pathology, Boston Children's Hospital, Bader 139.1, BCH 3027, 300 Longwood Ave, Boston, MA 02115; e-mail: mark.fleming@childrens.harvard.edu.

## Footnote

The online version of this article contains a data supplement.

## REFERENCES

1. Finberg KE, Heeney MM, Campagna DR, et al. Mutations in *TMPRSS6* cause iron-refractory iron deficiency anemia (IRIDA). *Nat Genet*. 2008;40(5):569-571.
2. Du X, She E, Gelbart T, et al. The serine protease *TMPRSS6* is required to sense iron deficiency. *Science*. 2008;320(5879):1088-1092.
3. Ganz T, Olbina G, Girelli D, Nemeth E, Westerman M. Immunoassay for human serum hepcidin. *Blood*. 2008;112(10):4292-4297.
4. Girelli D, Nemeth E, Swinkels DW. Heparin in the diagnosis of iron disorders. *Blood*. 2016;127(23):2809-2813.
5. De Falco L, Silvestri L, Kannengiesser C, et al. Functional and clinical impact of novel *TMPRSS6* variants in iron-refractory iron-deficiency anemia patients and genotype-phenotype studies. *Hum Mutat*. 2014;35(11):1321-1329.
6. Donker AE, Schaap CC, Novotny VM, et al. Iron refractory iron deficiency anemia: a heterogeneous disease that is not always iron refractory. *Am J Hematol*. 2016;91(12):E482-E490.

DOI 10.1182/blood-2017-03-773028

© 2018 by The American Society of Hematology

## TO THE EDITOR:

# Hypoxia downregulates protein S expression

Vijaya S. Pilli,<sup>1</sup> Arani Datta,<sup>1\*</sup> Sadaf Afreen,<sup>1\*</sup> Donna Catalano,<sup>2</sup> Gyongyi Szabo,<sup>2</sup> and Rinku Majumder<sup>1</sup>

<sup>1</sup>Department of Biochemistry and Molecular Biology, LSU Health Sciences Center, New Orleans, LA; and <sup>2</sup>Department of Medicine, University of Massachusetts Medical School, Worcester, MA

Hypoxia is associated with an increased risk of thrombosis.<sup>1,2</sup> Hypoxia is usually caused by high altitude,<sup>3</sup> but it can be elicited by chronic alcoholism,<sup>4,5</sup> chronic smoking,<sup>6</sup> and clinical conditions such as lung failure,<sup>7,8</sup> sickle cell anemia,<sup>9</sup> and nonalcoholic

fatty liver disease.<sup>10</sup> Notably, deficiencies of protein S (PS), a natural anticoagulant that inhibits coagulation factor IXa, also occur in sickle cell anemia and at high altitude.<sup>11-16</sup> This later circumstance purports a possibility that hypoxia causes a PS

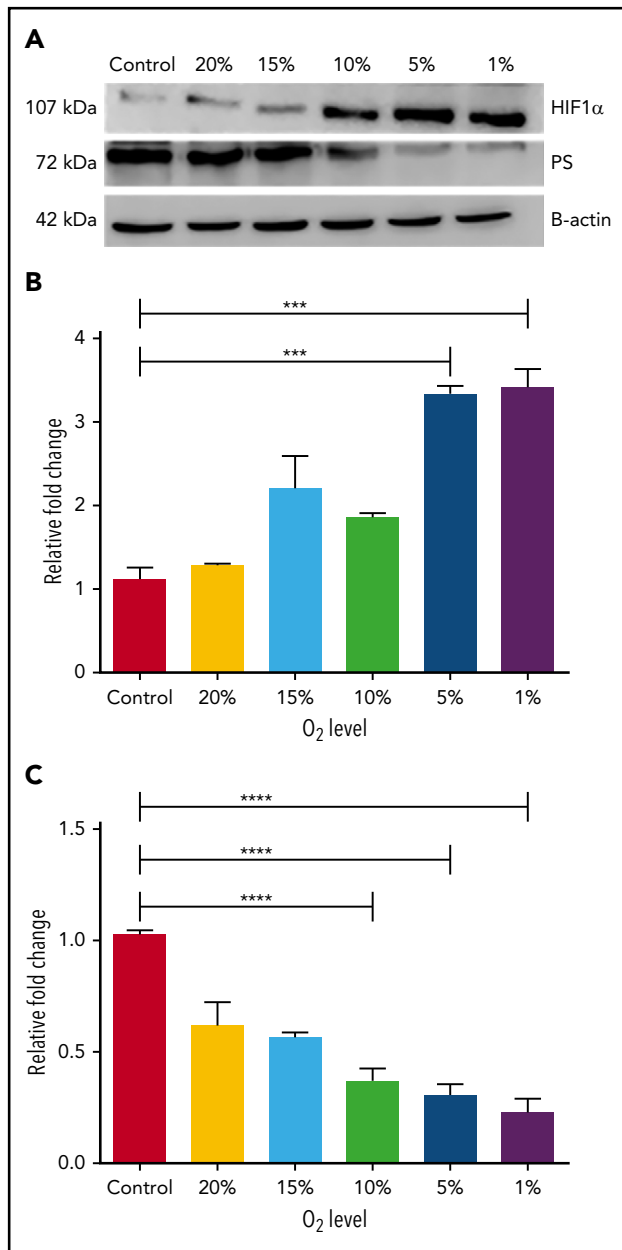


**Figure 1. HIF1 $\alpha$  downregulates PS expression in hypoxic HEPG2 cells.** (A) Representative immunoblots showing relative PS and HIF1 $\alpha$  protein levels in HEPG2 cells grown at different O<sub>2</sub> concentrations. (B) Relative HIF1 $\alpha$  mRNA levels in HEPG2 cells grown at different concentrations of O<sub>2</sub>. (C) Relative PS mRNA levels in HEPG2 cells grown at different concentrations of O<sub>2</sub>. \*\*\*\**P* < .0001.

deficiency, in turn, elevating thrombotic risk. The cellular response to hypoxia is mediated by the dimeric transcription factor hypoxia inducible factor 1 (HIF1). The HIF1 $\alpha$  subunit of HIF1 is expressed constitutively in many tissues, and an O<sub>2</sub>-dependent signaling system continuously degrades HIF1 $\alpha$ .<sup>17</sup> Conversely, O<sub>2</sub> deficiency prevents HIF1 $\alpha$  degradation and stabilizes HIF1 $\alpha$ .<sup>18</sup> In this study, we demonstrate that HIF1 downregulates PS expression, a finding that suggests a molecular link between hypoxia and thrombosis.

Because PS is produced primarily in liver, we used human hepatocarcinoma (HEPG2) cells, the standard cell system for studying PS expression.<sup>19</sup> We cultured HEPG2 cells at normoxia

(22% O<sub>2</sub>) and under hypoxic conditions ranging from 20% to 1% O<sub>2</sub>. PS levels were assessed by immunoblotting. Increasing hypoxia reduced PS protein level to 20% and concurrently increased HIF1 $\alpha$  stability (Figure 1A). We also measured by quantitative polymerase chain reaction (qPCR) the effect of hypoxia on transcription of HIF1 $\alpha$  (Figure 1B) and PS (Figure 1C). This analysis revealed that decreased O<sub>2</sub> levels enhanced HIF1 $\alpha$  transcription (from 100% to 340%). Conversely, a stepwise decrease in O<sub>2</sub> (from 20% to 1%) progressively downregulated PS transcription (from 100% to 20%). Notably, hypoxia had no measurable effect on transcription or expression of another natural anticoagulant, TFPI (supplemental Figure 1A-B, available on the Blood Web site).

The inverse relationship between HIF1 $\alpha$  and PS levels as a function of O<sub>2</sub> concentration suggested that HIF1 protein might regulate PS expression. We confirmed this conjecture by modulating HIF1 $\alpha$  expression in mouse liver. The HIF1 $\alpha$  P564A mutant (HIF1 $\alpha$  dPA) is resistant to degradation, resulting in sustained, elevated HIF1 protein abundance, even under normal O<sub>2</sub> concentrations. We collected liver samples from HIF1 $\alpha$  liver-specific knockout mice, knockout mice expressing HIF1 $\alpha$  dPA in the liver (gift from William Kim, University of North Carolina-Chapel Hill),<sup>20,21</sup> and control (nonknockout) mice and analyzed the samples by immunoblotting (in duplicate) and qPCR. Setting the control mice HIF1 expression levels at 100%, we found that the HIF1 $\alpha$  dPA mice had an expectedly high (~325%) HIF1 expression. Compared with control mice (100%), PS protein level in the liver from HIF1 $\alpha$  liver-specific knockout mice was elevated (~220%) and diminished in liver from HIF1 $\alpha$  dPA mice (~50%) (Figure 2A; supplemental Table 1). Likewise, we observed corresponding alterations in PS transcription. Compared with control mice, PS messenger RNA (mRNA) increased by twofold ( $\pm 0.25$ ) in HIF1 $\alpha$  knockout mice, and PS mRNA was reduced to 0.3-fold ( $\pm 0.15$ ) in HIF1 $\alpha$  mice that expressed HIF1 $\alpha$  dPA (Figure 2B).

Liver-specific HIF1 $\alpha$  alterations showed immediate effects on plasma PS levels. PS levels increased by 2 ( $\pm 0.4$ )-fold in plasma from HIF1 $\alpha$  knockout mice, whereas PS was reduced by 2 ( $\pm 0.12$ )-fold in plasma from HIF1 $\alpha$  dPA mice (Figure 2C). Changes in plasma PS were also reflected in the extent of thrombin generation. Plasma from HIF1 $\alpha$  knockout mice produced five-fold less thrombin than control mouse plasma, and plasma from HIF1 $\alpha$  dPA mice produced 1.5-fold more thrombin than control mice (Figure 2D). Data were analyzed by Graph-Pad Prism analysis software. Results were expressed as mean  $\pm$  SD, and *P* values are presented in the figures as \**P* < .01; \*\**P* < .001, \*\*\*\**P* < .0001.

To confirm that the variations in thrombin generation were due directly to changes in PS levels, we measured the effects of adding exogenous PS and a PS-specific antibody to plasmas from the aforementioned mice. Thrombin generation was not affected by supplementation of 450 nM anti-PS antibody into plasma from HIF1 $\alpha$  dPA mice, whereas 150 nM PS supplementation reduced thrombin generation by 25% (Figure 2E). Supplementation of control mouse plasma with exogenous PS decreased thrombin generation (Figure 2F), and addition of anti-PS antibody increased thrombin generation (Figure 2F). PS supplementation of plasma from HIF1 $\alpha$  knockout mice increased thrombin generation, whereas anti-PS antibody had no significant effect (Figure 2G). These results confirmed that the changes in plasma PS levels were

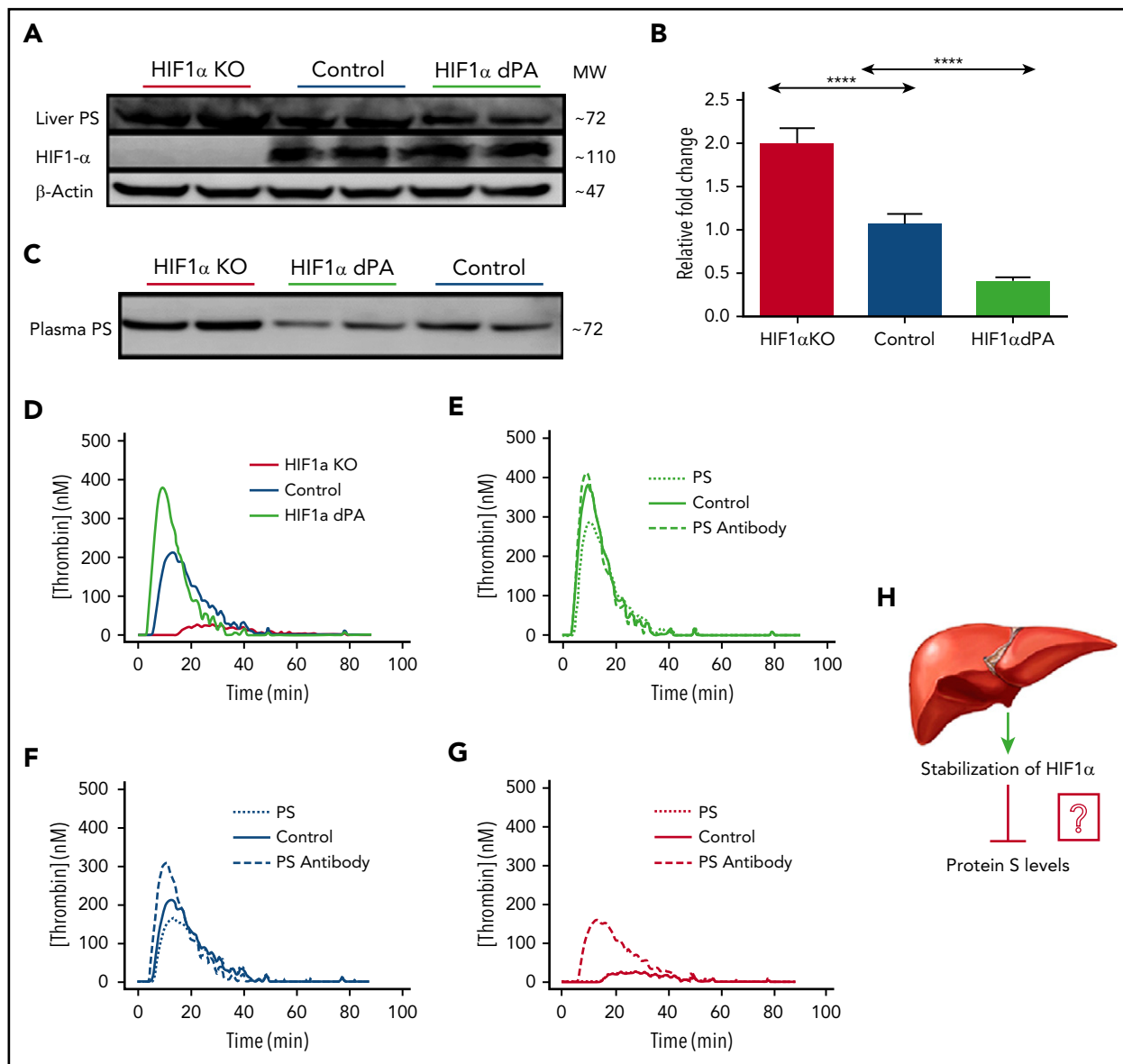


**Figure 2. HIF1 $\alpha$  regulates PS expression in the mouse liver.** (A) Representative immunoblots showing relative PS and HIF1 $\alpha$  protein levels in livers from HIF1 $\alpha$  liver-specific knockout mice, control mice, and liver-specific HIF1 $\alpha$  dPA mice. Each blot contained samples from 2 mice belonging to each category. The reported data are representative of 3 separate immunoblots, and the blot densities are quantified in supplemental Table 1. (B) Relative PS mRNA levels in the livers of control mice, HIF1 $\alpha$  liver-specific knockout (KO) mice, and liver-specific HIF1 $\alpha$  dPA mice (n = 5 per group). (C) Representative immunoblots assessing relative amounts of PS in plasmas from HIF1 $\alpha$  liver-specific knockout mice, liver-specific HIF1 $\alpha$  dPA mice, and control mice. (D) The graph shows relative thrombin generation by the plasmas from HIF1 $\alpha$  liver-specific knockout mice, control mice, and liver-specific HIF1 $\alpha$  dPA mice. (E) The graph shows thrombin generation by plasma from liver-specific HIF1 $\alpha$  dPA mice that was inhibited by addition of exogenous PS. (F) The graph shows relative thrombin generation from control mouse plasma following addition of anti-PS antibody or exogenous PS. (G) Thrombin generation by plasma from HIF1 $\alpha$  liver-specific knockout mice in the presence of PS or anti-PS antibody. (H) Model depicting stabilization of HIF1 $\alpha$  in mouse liver suppresses PS expression. \*\*\*\*P < .0001.

directly responsible for the variations in thrombin generation. We note that pathological stabilization of HIF1 $\alpha$  often occurs in cancer and metabolic disorders that are also associated with higher risks of thrombosis and increased procoagulant activity. The foregoing results demonstrating suppression of PS activity in mice with hyperstable HIF1 $\alpha$  dPA suggest a molecular explanation for increased thrombosis and procoagulant activity in cancer and other disorders.

## Conclusion

Our results show that stabilization of HIF1 in the liver, a normal response to hypoxia, is associated with reduced PS expression

that results in a lower plasma PS level (Figure 2H) and, in turn, increased likelihood of thrombosis. Although HIF1 is a well-documented, general transcriptional activator, it has also been identified as a transcriptional repressor. For example, HIF1 interacts with genes such as AIF,<sup>22</sup> cyclin D1,<sup>23</sup> and Bid<sup>24</sup> and reduces their transcription under hypoxia. In addition, HIF1 $\alpha$  regulates transcription of a variety of microRNAs that, in turn, regulate expression of various target mRNAs<sup>25</sup>; in these cases, HIF1 can be said to be an indirect transcriptional regulator of these mRNAs. The ease of culture of HEPG2 cells compared with normal hepatocytes offers a useful in vitro model for future studies of HIF1 in PS gene regulation. We have demonstrated a reciprocal relationship between the expression of HIF1

and PS. We will next determine whether HIF1-mediated PS downregulation occurs by a direct or indirect HIF1 transcriptional repressor function. This study will open a new direction for targeting hypoxia-mediated thrombotic disorders.

The aforementioned study is approved by Institutional Biosafety Committee (16400) and Institutional Animal Care and Use Committee (3504) of LSU Health Science Center.

## Acknowledgments

The authors thank Fokhrul Hossain and Samarpan Majumder (Department of Genetics, LSU Health Science Center) for help with qPCR figures.

This work was funded by the LSU Health Science Center Special Appropriation Award (0101500039) (R.M.) and National Institutes of Health, National Heart, Lung, and Blood Institute grant 1R01 HL 118557-01A1-07.

## Authorship

Contribution: V.S.P. and R.M. contributed to study design; V.S.P., S.A., and A.D. collected and analyzed experimental data; D.C. and G.S. maintained the mice and collected liver and plasma samples; V.S.P. wrote the initial version of the manuscript; A.D. assisted in revision of the manuscript; and R.M. conceived the study, interpreted the results, and wrote the final version of the manuscript.

Conflict of interest disclosure: The authors declare no competing financial interests.

ORCID profiles: A.D., 0000-0002-2459-5964; R.M., 0000-0002-1727-7220.

Correspondence: Rinku Majumder, Room 7114, Medical Education Building, 1901 Perdido St, New Orleans, LA 70112; e-mail: rmajum@lsuhsc.edu.

## Footnotes

\*A.D. and S.A. contributed equally to this study.

The online version of this article contains a data supplement.

There is a *Blood* Commentary on this article in this issue.

## REFERENCES

1. Brill A, Suidan GL, Wagner DD. Hypoxia, such as encountered at high altitude, promotes deep vein thrombosis in mice. *J Thromb Haemost*. 2013;11(9):1773-1775.
2. Zangari M, Fink L, Tolomelli G, et al. Could hypoxia increase the prevalence of thrombotic complications in polycythemia vera? *Blood Coagul Fibrinolysis*. 2013;24(3):311-316.
3. Grocott M, Montgomery H, Vercueil A. High-altitude physiology and pathophysiology: implications and relevance for intensive care medicine. *Crit Care*. 2007;11(1):203.
4. Arteel GE, Raleigh JA, Bradford BU, Thurman RG. Acute alcohol produces hypoxia directly in rat liver tissue in vivo: role of Kupffer cells. *Am J Physiol*. 1996;271(3 Pt 1):G494-G500.
5. Bailey SM, Mantena SK, Millender-Swain T, et al. Ethanol and tobacco smoke increase hepatic steatosis and hypoxia in the hypercholesterolemic apoE(-/-) mouse: implications for a "multihit" hypothesis of fatty liver disease. *Free Radic Biol Med*. 2009;46(7):928-938.
6. Fricker M, Goggins BJ, Mateer S, et al. Chronic cigarette smoke exposure induces systemic hypoxia that drives intestinal dysfunction. *JCI Insight*. 2018;3(3):94040.
7. Tuder RM, Yun JH, Bhunia A, Fijalkowska I. Hypoxia and chronic lung disease. *J Mol Med (Berl)*. 2007;85(12):1317-1324.
8. Weng T, Karmouty-Quintana H, Garcia-Morales LJ, et al. Hypoxia-induced deoxycytidine kinase expression contributes to apoptosis in chronic lung disease. *FASEB J*. 2013;27(5):2013-2026.
9. Sun K, Xia Y. New insights into sickle cell disease: a disease of hypoxia. *Curr Opin Hematol*. 2013;20(3):215-221.
10. Lin Q-C, Chen L-D, Chen G-P, et al. Association between nocturnal hypoxia and liver injury in the setting of nonalcoholic fatty liver disease. *Sleep Breath*. 2015;19(1):273-280.
11. Chattopadhyay R, Sengupta T, Majumder R. Inhibition of intrinsic Xase by protein S: a novel regulatory role of protein S independent of activated protein C. *Arterioscler Thromb Vasc Biol*. 2012;32(10):2387-2393.
12. Francis RB Jr. Protein S deficiency in sickle cell anemia. *J Lab Clin Med*. 1988;111(5):571-576.
13. Nair V, Mohapatro AK, Sreedhar M, et al. A case of hereditary protein S deficiency presenting with cerebral sinus venous thrombosis and deep vein thrombosis at high altitude. *Acta Haematol*. 2008;119(3):158-161.
14. Plautz WE, Sekhar Pilli VS, Cooley BC, et al. Anticoagulant protein S targets the factor IXa heparin-binding exosite to prevent thrombosis. *Arterioscler Thromb Vasc Biol*. 2018;38(4):816-828.
15. Prince R, Bologna L, Manetti M, et al. Targeting anticoagulant protein S to improve hemostasis in hemophilia. *Blood*. 2018;131(12):1360-1371.
16. Sekhar S, Plautz W, Majumder R. The journey of protein S from an anticoagulant to a signaling molecule. *JSM Biochem Mol Biol*. 2016;3(1):1014.
17. Semenza GL. Hypoxia-inducible factor 1 (HIF-1) pathway. *Sci STKE*. 2007;407:cm8.
18. Ginouvès A, Ilc K, Macías N, Pouyssegur J, Berra E. PHDs overactivation during chronic hypoxia "desensitizes" HIF1 $\alpha$  and protects cells from necrosis. *Proc Natl Acad Sci USA*. 2008;105(12):4745-4750.
19. Suzuki A, Sanda N, Miyawaki Y, et al. Down-regulation of PROS1 gene expression by 17 $\beta$ -estradiol via estrogen receptor  $\alpha$  (ER $\alpha$ )-Sp1 interaction recruiting receptor-interacting protein 140 and the corepressor HDAC3 complex. *J Biol Chem*. 2010;285(18):13444-13453.
20. Nath B, Levin I, Csak T, et al. Hepatocyte-specific hypoxia-inducible factor-1 $\alpha$  is a determinant of lipid accumulation and liver injury in alcohol-induced steatosis in mice. *Hepatology*. 2011;53(5):1526-1537.
21. Kim WY, Safran M, Buckley MR, et al. Failure to prolyl hydroxylate hypoxia-inducible factor alpha phenocopies VHL inactivation in vivo. *EMBO J*. 2006;25(19):4650-4662.
22. Xiong Z, Guo M, Yu Y, et al. Downregulation of AIF by HIF-1 contributes to hypoxia-induced epithelial-mesenchymal transition of colon cancer. *Carcinogenesis*. 2016;37(11):1079-1088.
23. Wen W, Ding J, Sun W, et al. Suppression of cyclin D1 by hypoxia-inducible factor-1 via direct mechanism inhibits the proliferation and 5-fluorouracil-induced apoptosis of A549 cells. *Cancer Res*. 2010;70(5):2010-2019.
24. Erler JT, Cawthorne CJ, Williams KJ, et al. Hypoxia-mediated down-regulation of Bid and Bax in tumors occurs via hypoxia-inducible factor 1-dependent and -independent mechanisms and contributes to drug resistance. *Mol Cell Biol*. 2004;24(7):2875-2889.
25. Hwang HW, Baxter LL, Loftus SK, et al. Distinct microRNA expression signatures are associated with melanoma subtypes and are regulated by HIF1A. *Pigment Cell Melanoma Res*. 2014;27(5):777-787.

DOI 10.1182/blood-2018-04-841585

© 2018 by The American Society of Hematology